Quantifying how urban landscape heterogeneity affects land surface temperature: A comparison of discrete and continuous approaches

ehsan Rahimi (ehsanrahimi666@gmail.com)
Shahid Beheshti University https://orcid.org/0000-0002-8401-472X
Shahindokht Barghjelveh
Shahid Beheshti University
Pinliang Dong
UNT: University of North Texas

Research Article

Keywords: Land Surface Temperature, Landscape Heterogeneity, Local Spatial Autocorrelation Indices, Texture-Based Measures, Landscape Metrics

Posted Date: March 15th, 2021

DOI: https://doi.org/10.21203/rs.3.rs-311911/v1

Quantifying how urban landscape heterogeneity affects land surface temperature: A comparison of discrete and continuous approaches

Ehsan Rahimi[1*], Shahindokht Barghjelveh[2], Pinliang Dong[3]

1 Environmental Research Institute, Shahid Beheshti University, Iran

2 Department of Geography and the Environment, University of North Texas, USA

Corresponding Author*: Ehsan Rahimi (E-mail: ehsanrahimi666@gmail.com)

Abstract

The present study examines the efficiency of discrete and continuous approaches to measuring urban heterogeneity effects on land surface temperature (LST). In the discrete approach, landscape metrics have been widely applied to quantifying the relationship between land surface temperature and urban spatial patterns and have received acceptable verification from landscape ecologists but some studies have shown their inaccurate results. The objective of the study is to compare landscape metrics and alternative approaches to measuring urban heterogeneity effects on LST. We compared landscape metrics results with nine texture-based measures, and two local spatial autocorrelation indices (local Moran's I and Gi statistics) applied to NDVI and BAI indices as a proxy of the spatial patterns of Tehran vegetation and built-up classes. The statistical results showed that urban landscape heterogeneity had significant impacts on the LST variations, and there was a compatibility between landscape metrics and alternative measures results. Overall results showed that the less-fragmented, the more complex, larger, and the higher number of patches, the lower LST. The most significant relationship was between patch density (PD) and LST (r= -0.71). Higher values of PD have mostly been interpreted to show higher fragmentation, but other landscape metrics and alternative measures declined this conclusion. Our study demonstrated that PD was not a reliable metric and presented no information about the spatial distribution of landscape elements. This study confirms alternative measures for overcoming landscape metrics shortcomings in estimating the effects of landscape heterogeneity on LST variations and gives land managers and urban planners new insights into the urban design.

Keywords: Land Surface Temperature, Landscape Heterogeneity, Local Spatial Autocorrelation Indices, Texture-Based Measures, Landscape Metrics.

Introduction

Land surface temperature (LST) of cities is warmer than suburbs due to impervious surfaces and buildings (Li et al., 2012; Tuttle et al., 2006). This phenomenon is due to the change of natural habitats into cities, parking lots, roads, and other impervious surfaces that considerably affect the local weather. A combination of natural and anthropogenic covers in cities results in a high heterogeneity. This heterogeneity affects the ecological processes and biodiversity of urban areas, which ultimately change the urban ecosystems functioning (Cushman and Huettmann, 2010). Numerous studies have estimated the relationship between LST and urban landscape heterogeneity, especially green spaces (Asgarian et al., 2015; Chen et al., 2014; Connors et al., 2013; Li et al., 2012; Sahana et al., 2016; Zhang et al., 2009; Zhang et al., 2013; Zheng et al., 2014). Nowadays, it is well-known that increasing the area of green spaces reduces LST values (Essa et al., 2013; Mallick et al., 2013; Yue et al., 2007; Zheng et al., 2014), but there are conflicting results about how the spatial arrangement of these green spaces affect LST. Some studies have claimed that higher fragmentation of green spaces positively affects LST (Bao et al., 2016; Li et al., 2011; Maimaitiyiming et al., 2014), whereas other studies have shown a negative effect (Kong et al., 2014; Masoudi and Tan, 2019; Masoudi et al., 2019; Xie et al., 2013).

Estimating the relationship between LST and green spaces patterns is an essential step for lowering LST in a city because it is possible to reduce the city's temperature by creating new green space patches. Therefore, there is an urgent need for quantifying the effects of urban landscape heterogeneity on LST correctly (Cadenasso et al., 2007). In this regard, Landscape metrics (McGarigal et al., 2002) and land use maps have frequently been used to investigate the relationship of urban heterogeneity and LST variations in the last years. This kind of discrete model has shown a sufficient capability to measure landscape structure patterns in many studies (Li et al., 2011; Liu and Weng, 2008). However, one of the problems of discrete methods is the errors related to the land use classification that are inevitable and may lead to unreal results (Shao and Wu, 2008). Therefore, the uncertainties related to the classification process of continuous variables into discrete classes, have reduced the efficiency and accuracy of these metrics (Dormann, 2007). Many other factors affect the accuracy and applicability of landscape metrics, like data source accuracy, scale effects, and ecological interpretation (Liu et al., 2013). It has also been reported that although some landscape metrics calculated differently, they are highly correlated (Neel et al., 2004; Turner et al., 2001).

As mentioned above, the accuracy of landscape metrics is considerably related to the accuracy of classified maps. The classification of urban areas that are a mixture of different covers is more complicated than other land covers. Therefore, we need new methods to examine urban heterogeneity correctly. One of the suggested alternative methods that can display and analyze urban heterogeneity based on continuous data (e.g., NDVI) are local spatial autocorrelation indices (e.g., local Moran's I and local Getis-Ord (Gi)). The Gi index in measuring urban fragmentation (Fan and Myint, 2014) and quantifying the effects of spatial patterns of green spaces on air temperature (Yang and Li, 2012) has shown significant ability. A few studies have applied local spatial autocorrelation to estimate the relationship between urban heterogeneity and LST (Fan et al., 2015; Jamei et al., 2019; Zheng et al., 2014). For instance, Fan et al. (2015), using spatial autocorrelation indices, showed that clustered or less fragmented patterns of grass or trees reduced LST.

Other alternative measures are texture-based measures that, similar to local spatial autocorrelation indices directly use remote sensing data as their inputs to capture landscape heterogeneity. These measures quantify spatial aspects of landscapes based on the gray-level co-occurrence matrix (GLCM) (Haralick and Shanmugam, 1973). Each GLCM index can highlight a particular property of texture, such as smoothness or coarseness produced by the uniformity or variability of image color or tone (Li and Narayanan, 2004; Park and Guldmann, 2020). Texture analysis methods have been used in the different remote sensing-based analysis, such as analysis of urban growth (Gluch, 2002), forest cover classification (Coburn and Roberts, 2004), habitat selection (Tuttle et al., 2006), and as a predictor of spices richness (Hofmann et al., 2017; Tuanmu and Jetz, 2015). Recent studies have paid attention to these indices and acknowledged their efficiency in measuring landscape heterogeneity. For example, Park and Guldmann (2020) compared the GLCM indices' ability as continuous metrics and landscape metrics as discrete metrics in estimating spatial patterns of tree canopy at the landscape level. They showed that there was a strong relationship between landscape characteristics resulted from GLCM indices and discrete models (landscape metrics).

Given the above background, this study aims to Compare landscape metrics and alternative measures (i.e. local spatial autocorrelation indices and texture-based measures) in determining the effects of urban heterogeneity on LST. In the present study, we first estimate land surface temperature changes in Tehran city between the years 2000 and 2017 using Landsat images. Next, we estimate the effects of urban composition and configuration on LST values using landscape metrics, spatial autocorrelation indices, and texture-based measures and compare the ability of these metrics in quantifying the relationship between LST and urban structure elements like buildings and green spaces.

Methods

Study area

Tehran has experienced the fastest population growth among the other cities in Iran. Tehran, with an area of 750 km^2, is a metropolis of 10 million inhabitants and locating on the southern side of the Alborz (a mountain range in northern Iran) (Sodoudi et al., 2014) (Fig. 1). This city divides into 22 areas and each area has its municipal administration that tries to provide adequate services to citizens. These 22 areas are different in size, amount of green spaces, paved surface, and buildings; hence, there are significant variations in LST temperatures of them. The annual mean temperature changes between 15°C and 18°C, and given the parts of different heights, there is a three Celsius difference in other districts' temperature.

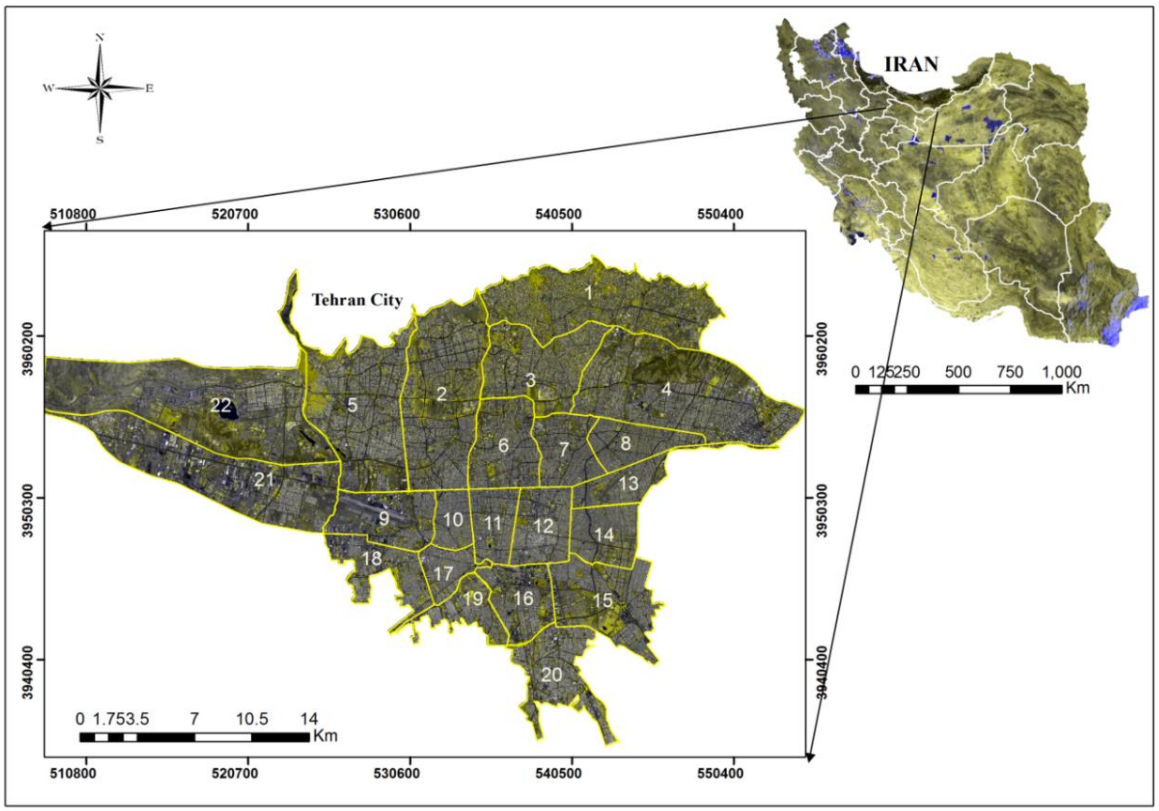

Fig.1. Study area location in Tehran province and Iran.

Spatial data

We used two Landsat image sets as initial data for deriving LST; Landsat 7 ETM^{+} image (band 6) on 15 May 2000, and Landsat 8 TIRS sensor on 22 May 2017 that has two TIR bands (band 10 and 11). To compare landscape metrics with texture measures and local spatial autocorrelation indices in measuring LST changes, two classified maps were derived from Landsat data in the years 2000 and 2017 using the maximum likelihood algorithm. The study area was classified into five classes, including green spaces (trees, parks, and natural vegetation covers), built-up areas, impervious surfaces (roads, parking areas, and cement surfaces), bare soils (useless lands without vegetation cover), and water (artificial lakes). All images were acquired during the growing season and are freely available at the Landsat archive at the United States Geological Survey (USGS) (http://glovis.usgs.gov).

Calculation of LST

We used the split-window method for Landsat 8 TIRS (Sahana et al., 2016) and the spectral radiance method for Landsat 7 ETM+ to retrieve Tehran LST maps (Equation 1).

$$L_\lambda = \frac{(L_{max} - L_{min})}{(QCAL_{max} - QCAL_{min})}(DN - QCAL_{min}) + L_{min} \quad (1)$$

Spectral Radiance to Temperature in Kelvin calculated as (Equation 2):

$$T_B = \frac{K_2}{ln\left(\frac{K_1}{L} + 1\right)} \quad (2)$$

LST for Landsat 8 TIRS calculated as follow (Equation 3);

$$LST = TB_{10} + C_1(TB_{10} - TB_{11}) + C_2(TB_{10} - TB_{11})^2 + C_0 + (C_3 + C_4W)(1 - \varepsilon) + (C_5 + C_6W)\Delta\varepsilon \quad (3)$$

Based on the equation below, we converted TB_{10} and TB_{11} to Top Atmospheric Spectral Radiance (Equation 4);

$$TOA = M_L \times DN + A_L \quad (4)$$

The Brightness temperature (T_B) for TB_{10} and TB_{11} bands calculated based on the following formula (Equation 5);

$$T_B = \frac{K_2}{ln\left(\frac{K_1}{TOA} + 1\right)} \quad (5)$$

Table. 1. Elements of LST equations and their explanations

Elements	Explanation
λ	TIR band 6
L_λ	Top of Atmosphere (TOA) radiance
$QCAL_{min}$	1
$QCAL_{max}$	255
L_{min}	1.238
L_{max}	15.303
L	Spectral Radiance
K_1	Calibration Constant = 607.76
K_2	Calibration Constant = 1260.56
TB	Surface Temperature
LST	Land surface temperature
TB_{10}	The brightness temperature of band 10
TB_{11}	The brightness temperature of band 11
ε	Mean band 10 and band 11
W	The atmospheric water vapor content
$\Delta\varepsilon$	Difference in LSE
DN	Digital number
TB	The Brightness temperature for both 10 and 11
TOA	Atmospheric spectral radiance

Table 2. Split window constant-coefficient values

Constant	Value
C0	-0.268
C1	1.378
C2	0.183
C3	54.3
C4	-2.238
C5	-129.2

C6	16.4

Table 2. Thermal constant values for TIR bands

Constant	BAND 10	BAND 11
K_1	1321.08	1201.14
K_2	777.89	480.89
Radiance multiplier (M_L)	0.0003342	0.0003342
Radiance add (A_L)	0.01	0.01

Landscape metrics

In this study, we applied landscape metrics to compare to local spatial autocorrelation indices and texture-based indices in estimating the relationship between urban landscape patterns and LST. For this purpose, eleven landscape metrics including, number of patches (NP), patch density (PD), percentage of landscape (PLAND), large patch index (LPI), effective mesh size (MESH), edge density (ED), total edge (TE), perimeter-area fractal dimension (PAFRAC) and splitting index (SPLIT), aggregation index (AI), and landscape shape index (LSI) (McGarigal et al.) were calculated using Fragstats software at class and landscape levels (Table 4).

Table 4. Descriptions of the selected landscape metrics.

Category	Metric	Equation	Range
Area and Edge			
	PLAND	$\frac{\sum a_{ij}}{A}(100)$	$0 \le PLAND \le 100$
	LPI	$\frac{max a_{ij}}{A}(100)$	$0 \le LPI \le 100$
	TE	$\sum e_{ik}$	$TE \ge 0$, without limit.
	ED	$\frac{\sum e_{ik}}{A}(10000)$	$0 \le ED$, no limit
Shape	PAFRAC	$\frac{2}{\frac{[(\sum lnp_{ij} - lna_{ij})] - [(\sum lnp_{ij})(\sum lna_{ij})]}{(\sum lnp_{ij}^2) - (\sum lnp_{ij})}}$	$1 \le PAFRAC \le 2$
Aggregation	LSI	$\frac{0.25\sum e_{ik}}{\sqrt{A}}$	$1 \le LSI$, no limit
	SPLIT	$\frac{A^2}{\sum A_{IJ}^2}$	$1 \le SPLIT \le$ number of cells in the landscape area squared
	MESH	$\frac{\sum A_{IJ}^2}{A}\left(\frac{1}{10000}\right)$	the ratio of cell size to landscape area $\le$ MESH $\le$ total landscape area (A)
	NP	n_I	$NP \ge 1$, without limit
	PD	$\frac{n_i}{A}(10000)(100)$	$PD > 0$, constrained by cell size.
	AI	$\left(\frac{g_{ii}}{max \rightarrow g_{ii}}\right)(100)$	$0 \le AI \le 100$

Note a_{ij}=area (m^2) of patch; A=total landscape area (m^2); n_i=number of class i patches in the landscape; e_{ij}=total length (m) of edges of patch ij, including landscape boundary, c = area (m^2) within patch ij separated from its boundary by a user-specified buffer width (m); g_{ii} = the number of adjacencies (contiguity) between pixels of patch class i; max g_{ii} =maximum possible number of adjacencies among pixels of patches of class i, h_{ij} = distance (m) from patch ij to the nearest neighboring patch of the same type (class), based on patch edge-to-edge distance, computed from cell center to cell center (McGarigal et al., 2002).

Local spatial autocorrelation indices

Spatial autocorrelation is an indicator that measures a phenomenon in which closely related observations are more similar than those that are farther away (Bolliger et al., 2007). The global spatial autocorrelation indices measure the total amount of data correlation across the study area, Local indicators of spatial autocorrelation allow us to locate clustered pixels by measuring how many features inside the fixed neighborhood are homogeneous (Anselin, 1995). In this study, we used Getis–Ord Local (Gi) (Getis and Ord, 1992) that compares pixel values at a

given location with those pixels at a lag, *d,* from the original pixel at location *i*. The function by Getis and Ord (1992) represented by the following equation (Equation 6):

$$G_i(d) = \frac{\sum_{i=1}^{n} w_i(d)x_i - x_i \sum_{i=1}^{n} w_i(d)}{S_{(i)}\sqrt{[(N-1)\sum_{i=1}^{n} w_i(d) - (\sum_{i=1}^{n} w_i(d))^2]/N-2}} \quad 6$$

Where *N* is the total pixel number, *Xi* and *Xj* are intensities in points *i* and *j* (with *I≠j*), *wij* (*d*) represents a weight that varies according to distance. The high values of the index show hot spots, while low values indicate cold spots (Lanorte et al., 2013).

The local Moran's I differ from the Getis statistic in that the co-variances than the sums are computed (Anselin, 1995). The local Moran's I is (Equation 7):

$$I_i = \frac{(X_i - \overline{X})}{{S_x}^2} \sum_{i=1}^{N} (w_{ij}(X_i - \overline{X})) \quad 7$$

Vegetation indices

In the continuous framework, we need to use continuous indices that reflect landscape patterns for measuring landscape fragmentation. In this regard, we used two normalized index images (NDVI and BAI) as alternative indicators of landscape patterns. The normalized difference vegetation index (NDVI) is useful for identifying green vegetation biomass (Fan and Myint, 2014), and is the most widely used index for many different applications, ranging from vegetation monitoring to urban sprawl (Nolè et al., 2014). The Built-up Areas Index (BAI) is one of the useful indexes for the study of urban phenomena that identifies waterproof surfaces like asphalt and concrete (Nolè et al., 2014). Values generated using the BAI index range from zero to one. The equations for calculating NDVI, BAI indices are as follow (Equations 8 and 9);

$$\text{NDVI} = \frac{R_{NIR} - R_{RED}}{R_{NIR} + R_{RED}} \quad 8$$

$$\text{BAI} = \frac{R_{BLUE} - R_{NIR}}{R_{BLUE} + R_{NIR}} \quad 9$$

Texture- based measures

We applied two types of texture measures to NDVI and BAI indices as input images: first and second-order measures (Table 5). The first-order measures describe the frequency distribution of pixels without regarding the pixel of neighbors. The second-order measures are based on the probability of observing a pair of values at two pixels within a specific distance (Tuanmu and Jetz, 2015). Fourteen measures of texture derived from the GLCM. In this study, we used eight measures including, entropy, homogeneity, contrast, energy, dissimilarity, correlation, mean, and variance (Table 5). Pearson correlation and regression analysis were used to estimate the relationship between texture measures and LST maps.

Table. 5. Texture metrics considered as measures of spatial landscape heterogeneity

Metric	Value range	Expected relationship*	Equation
First-order texture			
Variance	≥ 0	$H \sim X$	$\sum_{i}^{N_g}\sum_{j}^{N_g}(i-\mu)^2 p(i,j)$
Mean	≥ 0	$H \sim X$	$\sum_{k}^{N_g} k p_{x-y}(k)$
Second-order texture			
Contrast	≥ 0	$H \sim X$	$\sum_{i}^{N_g}\sum_{j}^{N_g}(i-j)^2 p_d(i,j)$
Dissimilarity	≥ 0	$H \sim X$	$\sum_{i}^{N_g}\sum_{j}^{N_g} p(i,j)\lvert i-j\rvert$
Entropy	≥ 0	$H \sim X$	$-\sum_{i}^{N_g}\sum_{j}^{N_g} p(i,j) log[p(i,j)]$
Homogeneity	≥ 0; ≤ 1	$H \sim -X$	$\sum_{i}^{N_g}\sum_{j}^{N_g}\frac{1}{1+(i-j)^2} p_d(i,j)$
Correlation	≥ 0; ≤ 0	$H \sim -X$	$\sum_{i}^{N_g}\sum_{j}^{N_g} p_d(i,j)\frac{(i-\mu_x)(j-\mu_y)}{\sigma_x\sigma_y}$
Energy	≥ 0; ≤ 1	$H \sim -X$	$\sum_{i}^{N_g}\sum_{j}^{N_g} g_{ig^2}$

*$H \sim X$, larger values indicate greater heterogeneity; $H \sim -X$, lower values indicate greater heterogeneity.

Results and Discussion

LST maps and change detection

Fig. 2 shows the graph of the probability density function of LST maps from 2000 to 2017. According to this figure, the average temperature of Tehran city has increased from 37.8 to 40.4 between the years 2000 to 2017. Spatial-temporal distribution of surface temperature showed that the western parts of Tehran had the highest temperature of 48°C in 2000 and 57°C in 2017 (Fig 4-A and B); the reason is replacing vegetation covers with non-evaporating and impervious surfaces. The water bodies and green spaces in the northern parts of Tehran had the least temperature, ranging from 9°C in 2000 to 25°C in 2017. Visual interpretation of LST maps (Fig 4) confirmed earlier results as colder parts (blue) were located mostly in the north of Tehran, and warmer parts (red) covered western parts of the city.

Results of landscape metrics (Table 6) showed that the area of both built-up and green space classes increased between 2000 to 2017. The percentage of green space increased from eight to 12 percent of the total study area between 2000 to 2017, leading to decreasing LST. The built-up class has also been increased from 62 to 70 percent resulting in increasing LST values. Despite the increasing amount of green space in 2017, Fig. 2 shows that LST has been increased significantly, implying that the effects of urban growth are more substantial than green spaces in increasing LST in 2017. Landscape aggregation metrics (MESH and AI) showed that both built-up and green space classes were more clustered and aggregated in 2017; this phenomenon might increase LST values. This hypothesis has been discussed and appropriately analyzed in the next results sections based on landscape metrics, local spatial autocorrelation indices, and texture-based measures.

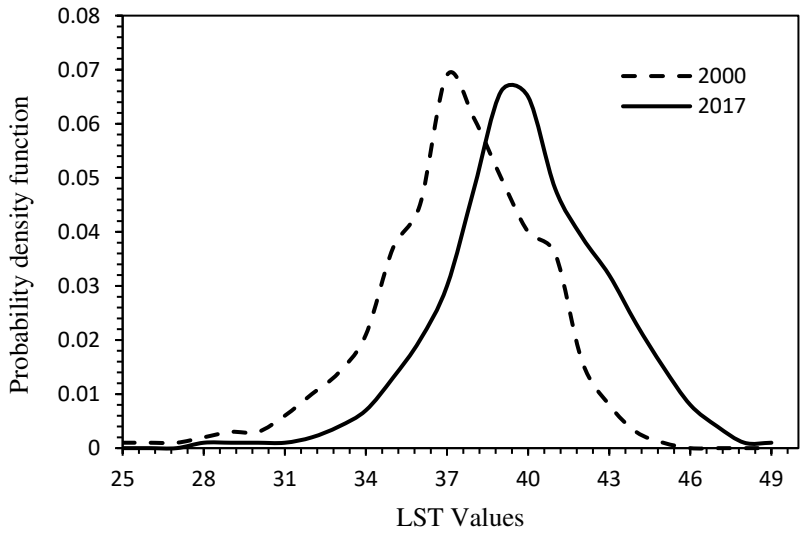

Fig. 2. Density function applied to LST maps in 2000 and 2017.

Table 6. Landscape metrics results for built-up and green space classes in different years.

	PLAND	NP	PD	LPI	ED	MESH	AI
Built-up 2000	62.06	862	1.42	25.21	93.09	6778.35	88.62
Built-up 2017	70.19	674	1.11	44.74	63.79	12704.87	93.06
Green space 2000	8.36	1687	2.78	2.97	36.90	55.35	67.06
Green space 2017	12.09	2023	3.34	0.89	33.45	9.629	79.18

Effects of landscape composition and configuration on LST

Fig. 5 shows the land cover map of Tehran city classified into five classes acquired from sentinel data in 2017. As mentioned above, 11 landscape metrics were calculated for the 22 municipal areas of Tehran city but only statistically significant results (P <= 0.1) were presented in Table 7. According to Fig. 5, most of the green spaces patches are located in the north and the west of Tehran, and less amount of this class is in the center and the south. Therefore, based on visual interpretation, there is an aggregated pattern of vegetation covers, mostly concentrated in the north of Tehran city. Consistent with several studies (Chen et al., 2014; Guo et al., 2019; Masoudi et al., 2019; Osborne and Alvares-Sanches, 2019; Zhou et al., 2011), our statistical results also showed that green space class had a more significant relationship with LST than other classes (Table. 7). Nevertheless, a few studies have shown that artificial elements correlate better with LST than vegetated surfaces (Liu et al., 2018).

Table 7. Pearson correlation coefficients and regression functions between landscape metrics of green space and LST in 2017.

Equation	r	R^2	P-value
LST= 43.07 - 0.07 PD*	-0.49	24.5%	0.09
LST= 41.44 - 0.14 PLAND	-0.58	34.1%	0.00
LST= 40.70 - 0.001 NP	-0.42	17.8%	0.05
LST= 42.30 - 0.16 PD	-0.71	51.7%	0.00
LST= 41.77 - 0.02 ED	-0.67	45.8%	0.00
LST= 57.24 - 12.10 PAFRAC	-0.38	14.6%	0.07
LST= 40.62 – 0.02 TE	-0.41	16.8%	0.05
LST= 41.13 - 0.03 LSI	-0.38	14.8%	0.07
LST= 39.67 + 0.042 SPLIT	0.38	14.5%	0.08

*Calculated at the landscape level

There was a significant difference between composition and configuration metrics in measuring the green space effects on LST in the present study. Similar to previous studies (Guo et al., 2019; Li et al., 2012) that showed increasing the area of green spaces resulted in decreasing LST, two metrics including the percentage of landscape (PLAND), and the number of patches (NP) of green space class were negatively correlated (-0.58 and -0.42 respectively) with LST. Chen et al. (2014) found that PLAND explained about 56% of the mean LST. Still, in the current study, PLAND demonstrated 34% of LST variations, implying that the configurational aspects of landscape structure were more capable to measure LST variations than compositional structure. Masoudi and Tan (2019) and Masoudi et al. (2019) found that area-related metrics (PLAND, LPI, AREA_AM, and MPS) were negatively correlated with LST for different understudy cities. Guo et al. (2019) observed a negative correlation of mean patch size (MPS) and the largest patch index (LPI) with LST that confirmed our results.

The most significant correlation was between patch density (PD) and LST (-0.71), apparently suggesting fragmented green space patches reduce LST. In several studies, higher LST has been associated with higher PD of green spaces, which is concluded to a more fragmented pattern (Fan et al., 2015; Li et al., 2012; Zhang et al., 2009; Zhou et al., 2011). However, McGarigal et al. (2002) frankly acknowledge that patch density (PD) has limited interpretive value by itself because it conveys no information about the sizes and configuration of patches, and selecting the neighbor rule for calculating PD affects the results. Jaeger (2000) also discussed the limitations of this metric for evaluating habitat fragmentation and concluded that PD behavior changes during the fragmentation process.

Interpreting results based on the PD metric does not always lead to an accurate conclusion. As mentioned earlier, this metric gives no information about the spatial aggregation of patches in a landscape (McGarigal et al., 2002). Masoudi and Tan (2019) and Masoudi et al. (2019) showed that PD was positively and AI negatively correlated with LST for all study areas and concluded that less fragmentation (lower PD) and higher aggregation resulted in cooling effects of urban green spaces. Positive impacts of aggregation have been reported in several studies (Estoque et al., 2017; Li et al., 2012; Xie et al., 2013; Zhang et al., 2009; Zheng et al., 2014; Zhibin et al., 2015), whereas Li et al. (2012), Maimaitiyiming et al. (2014) and Bao et al. (2016) showed negative impacts. For the built-up class, a more fragmented and edge-complicated pattern of unvegetated surfaces has been shown to have a warmer LST than vegetated surfaces (Zhou et al., 2011). Zhou et al. (2011) found a negative correlation between LST and patch density of paved surfaces and a positive correlation between LST and patch

density of buildings. They suggested that fragmented built-up class (higher PD) led to higher LST.

The earlier studies have concluded their results based on the belief that higher PD means higher fragmentation. Still, our research shows that this statement is not always accurate because the SPLIT (r= 0.38) metric and other aggregation metrics (CLUMPY, AI, and MESH) showed that less-fragmented and clustered vegetation cover in Tehran city resulted in lower LST not dispersed (Table. 7). SPLIT metric approaches 1 when the landscape; consists of a single patch and increases as the focal patch type increasingly losses its area and is subdivided into smaller patches (McGarigal et al., 2002). Therefore, Relationship between LST and aggregation metrics like SPLIT showed that fragmented green space affects LST adversely.

All shape complexity metrics (ED, TE, LSI, and PAFRAC) were negatively correlated with LST, consistent with many studies (Asgarian et al., 2015; Bao et al., 2016; Chen et al., 2014; Estoque et al., 2017; Guo et al., 2019; Li et al., 2012; Zhou et al., 2011), suggesting the positive effects of more complex shapes in reducing LST. Li et al. (2012) concluded that green spaces configuration metrics affected LST significantly, particularly for LSI and ED that were negatively correlated. Guo et al. (2019) also showed a positive effect of edge density (ED) on LST. They concluded that an increased edge density might enhance energy flow to surrounding areas, leading to decreased LST. However, Kong et al. (2014), Masoudi et al. (2019), Xie et al. (2013), and Masoudi and Tan (2019) indicated that shape complexity metrics (ED, LSI, SHAPE_AM, and FRAC_AM), especially ED and LSI of green spaces were positively correlated with LST in all cities under study, implying that the more complex shapes affected LST values negatively.

In the present study, landscape configuration was generally observed to have more significant effects on LST than Composition, similar results have been shown with several studies (Chen et al., 2014; Guo et al., 2019; Zhang et al., 2009). Statistical results of landscape metrics for green space class showed that less-fragmented (lower SPLIT), more complicated in shape (higher ED and LSI), larger, and the number of patches lead to lower LST.

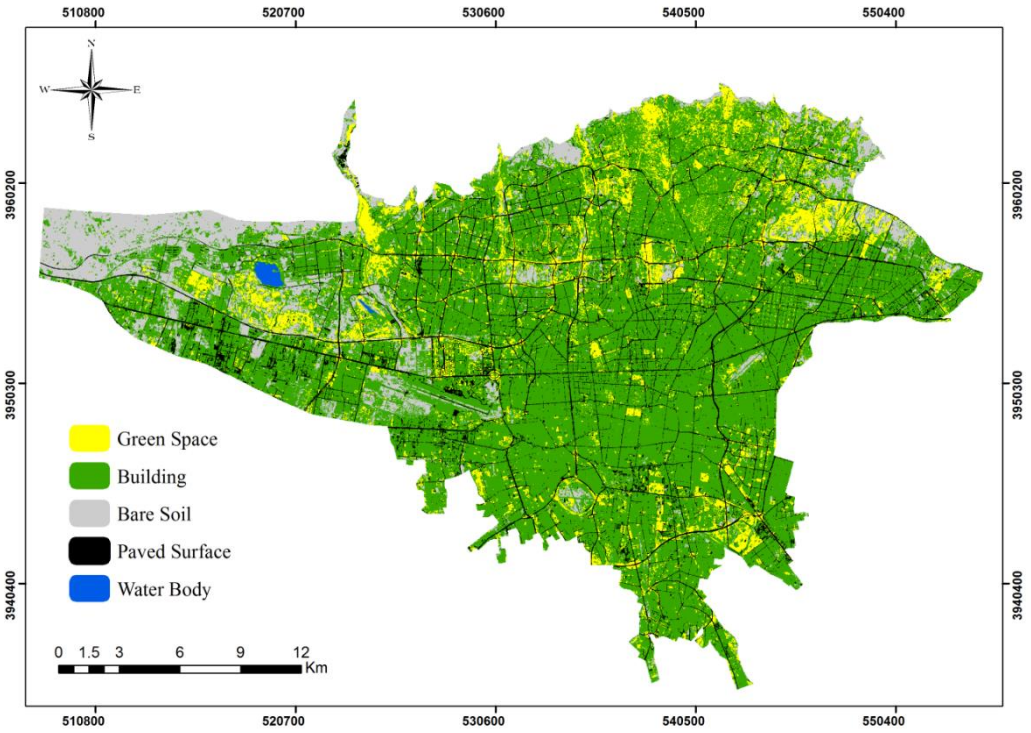

Fig. 3. Land cover map of the study area in 2017.

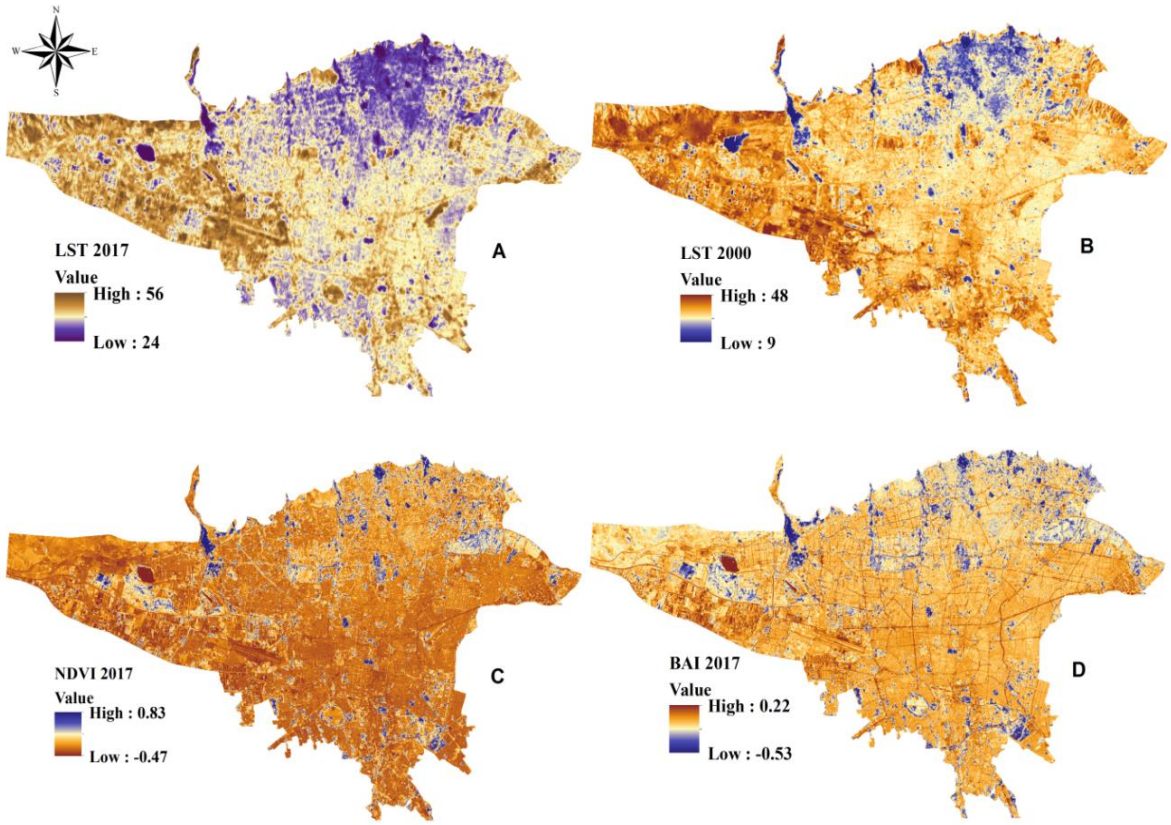

Fig. 4. LST maps in (A) 2017, (B) 2000, (C) NDVI, and (D) BAI indices.

Local spatial autocorrelation indices and LST

The statistical relationships between Local spatial autocorrelation indices and LST maps in the year 2017 are presented in Table 8. An area is interpreted as a clustered or homogeneous (high-value clustering or low-value clustering) when the local Moran's I is considerably higher than the mean. Heterogeneous regions are indicated by a significantly lower value of local Moran's I. Lower values of local Moran's I for NDVI and BAI indices show dispersed or heterogeneous pixels, and high values of this index show clusters of homogeneous cells (green space and built-up) (Fig 4-A and D). The negative relationship between local Moran's I of NDVI and LST (r= -0.60) implies that LST values increase as values of local Moran's I decrease or, in other words, clustered patterns of NDVI (green spaces) in Tehran city are cooler than heterogeneous ones. This result is consistent with landscape metrics that showed homogenous patterns of green space class were more correlated to LST than fragmented. For local Moran's I of BAI (r= -0.59) (Fig. 5), higher values belong to areas with the least vegetation cover and constitute evident clusters of buildings and paved surfaces. Therefore, a positive correlation between local Moran's I of BAI and LST shows that warmer places are in more clustered and more homogeneous buildings parts of Tehran city. It is essential to consider that local Moran's I is strongly affected by input images, meaning that high values of the input images are often considered as clustered patterns (Fig. 5).

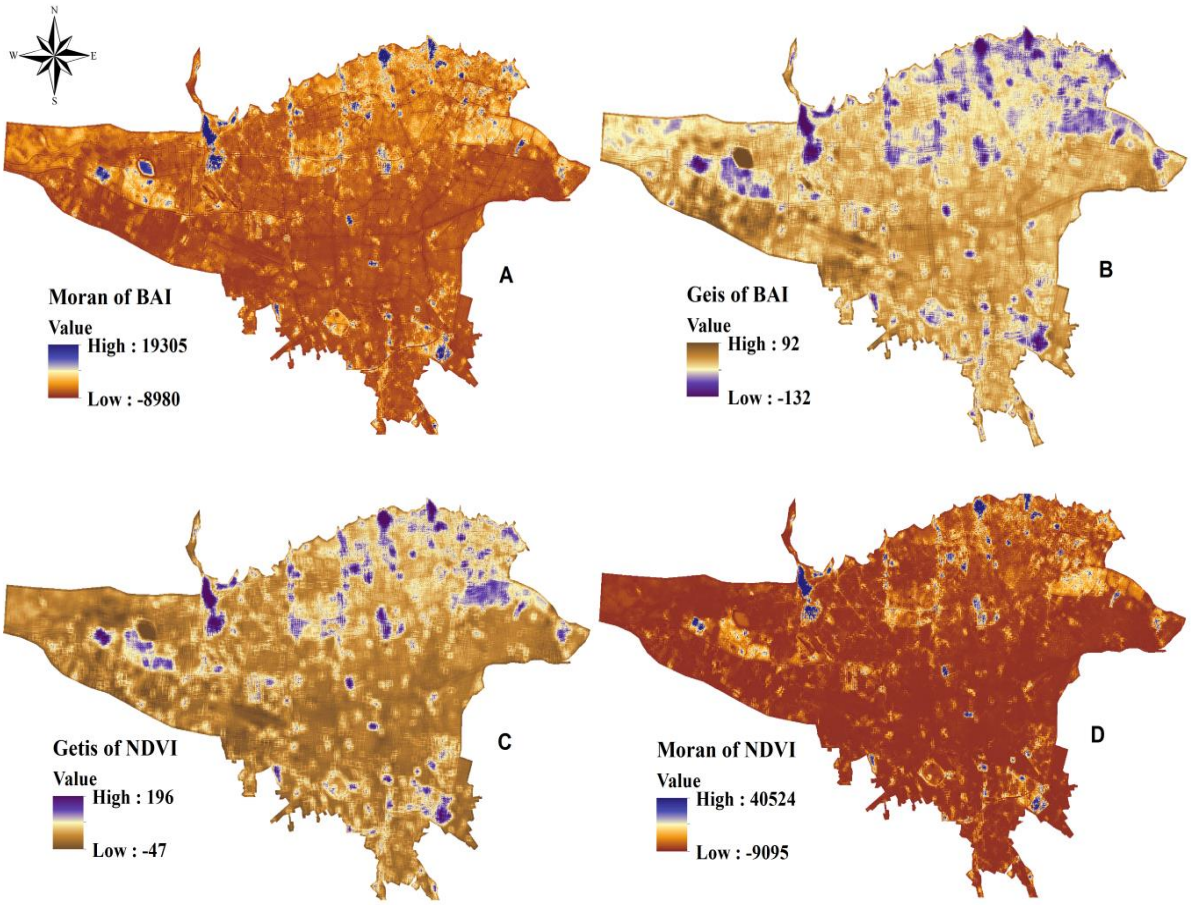

Fig.5. Local spatial autocorrelation indices applied to NDVI and BAI indices. (A) Moran of BAI, (B) Getis of BAI, (C) Getis of NDVI, and (D) Moran of NDVI.

In this part, our results are consistent with Fan et al. (2015) that showed clustered or less fragmented patterns of grass or trees reduced LST more effectively than dispersed patterns. Their results showed negative relationships between local Moran's I of vegetation and seasonal LST for both grass and trees, implying that less fragmented or clustered vegetation patterns effectively reduced urban temperatures. Zheng et al. (2014) also applied the local Moran's I for evaluating the relationship between buildings and paved surfaces with LST. They found that Local Moran's I of buildings had a weak correlation with LST (R^2 <0.04). In contrast, paved surfaces presented a stronger positive relationship (R^2 > 0.17), suggesting that spatial arrangements of buildings had a weak impact on temperature. The direct relationship between local Moran's I of paved surfaces, and LST indicated that the clustered patterns of paved surfaces tended to increase surface temperature than dispersed patterns (Zheng et al., 2014).

The Getis of NDVI (Fig 4-C) shows that the lower values of this index (cold spots) are mostly concentrated in the built-up regions where the vegetation covers are very sparse and the higher values (hot spots) are related to clustered vegetation covers. Both low and high values of the Getis index indicate a homogeneous landscape. In contrast, the Getis values around zero imply a maximum degree of landscape fragmentation and could be considered as the critical point for evaluating landscape heterogeneity (Fan and Myint, 2014). The Getis index determines the degree of dependency of LST to different covers that are not easy-classified using classification algorithms. In the current study, the Getis of NDVI and BAI showed more robust relationships with LST than the Local Moran's I. The Getis of NDVI had a negative correlation (-0.57), and the Getis of BAI showed a stronger positive relationship (r=0.68), suggesting that buildings affected LST more than vegetation clusters. Consistent with previous results, the Getis index also showed that more homogenous and less-fragmented green spaces decreased LST effectively than dispersed patterns. Jamei et al. (2019) also showed that the spatial patterns of LST were statistically significant in hot spot zones, which indicated the intensity of LST had a significant spatial cluster in Zhengzhou City. Overall, local Moran's I and Getis indices were consistent with the results of landscape metrics and showed homogenous patterns of green spaces lowered LST remarkably.

Table 8. The regression statistics and Pearson correlation coefficients of texture and autocorrelation indices with LST in 2017

Equation	r	R^2	P-value
LST= 44.17 - 37.63 NDVI	-0.67	44.9%	0.00
LST= 46.32 + 43.6 BAI	0.68	46.7%	0.00
LST= 35.47 + 0.04 Getis of BAI	0.68	46.2%	0.00
LST= 44.67 - 0.03 Getis of NDVI	-0.64	41.8%	0.00
LST= 36.548 + 0.001Moran of BAI	0.59	33.6%	0.00
LST= 42.09 - 0.03 Moran of NDVI	-0.60	35.4%	0.00
LST= 43.01 - 0.04 Contrast of NDVI	-0.63	39.8%	0.00
LST= 43.43 - 0.05 Contrast of BAI	-0.55	31.2%	0.00
LST= 44.75 - 0.04 Mean of NDVI	-0.65	43.5%	0.00
LST= 34.42 + 0.04 Mean of BAI	0.65	42.5%	0.00
LST= 30.89 + 0.08 Energy of NDVI	0.61	38.2%	0.01
LST= 26.27 + 0.11 Energy of BAI	0.53	28.8%	0.01
LST= 50.45 - 0.04 Entropy of NDVI	-0.50	33.9%	0.00
LST= 57.43 - 0.07 Entropy of BAI	-0.58	25%	0.01
LST= 42.90 - 0.05 Variance of BAI	-0.50	25.6%	0.00
LST= 42.37 - 0.03 Variance of NDVI	-0.53	28.8%	0.01
LST= 35.70 + 0.04 Homogeneity of NDVI	0.69	47.9%	0.01
LST= 34.84 + 0.05 Homogeneity of BAI	0.53	28.7%	0.01
LST= 32.19 + 0.04 Correlation of NDVI	0.44	20.2%	0.03
LST= 54.19 - 0.06 Correlation of BAI	-0.35	12.8%	0.01
LST= 44.02 - 0.04 Dissimilarity of NDVI	-0.65	43.1%	0.00
LST= 44.93 - 0.05 Dissimilarity of BAI	-0.57	33.4%	0.00

Estimating the relationship between texture measures and LST

Table 8 presents the results of the statistical relationship between LST and texture-based measures. Generally, these measures often have a high correlation with each other and can be divided into two groups based on measuring and displaying landscape heterogeneity; 1- measures that depict greater heterogeneity with higher values (e.g., mean, variance, contrast, dissimilarity, and entropy) and 2- measures that display greater heterogeneity with lower values (e.g. homogeneity, correlation, and energy). According to this classification, the interpretation of their results is similar for each group of measures. The first group (except for the mean of BAI) showed a negative correlation with LST, suggesting that greater heterogeneity of both NDVI and BAI led to higher LST. Results of the second group confirm previous results. For example, the homogeneity measure had the most significant relationship (R^2= 47.9%) with LST.

The lower values of homogeneity (Fig 6-D) index show the greater heterogeneity (Tuanmu and Jetz, 2015). Therefore, the positive correlation between the homogeneity of NDVI and LST (r= 0.69) implies that LST values increase when vegetation covers are fragmented and dispersed. This result is consistent with local spatial autocorrelation indices and landscape metrics, which indicated that clustered and homogeneous vegetation covers had lower LST values than dispersed patterns. Homogeneity of BAI also was positively correlated to LST, suggesting the more clustered buildings, the more increased LST. In the present study, texture measures had a stronger correlation with LST than local spatial autocorrelation indices, meaning that texture measures had a higher ability to show landscape heterogeneity than the other metrics examined in the study. Among all metrics used in this study for estimating the relationship between LST and landscape heterogeneity, the strongest one was homogeneity of NDVI (R^2= 47.9%) which was a second-order texture measure. Texture measures have been used in various studies and have shown acceptable ability in ecological studies (Hofmann et al.,

2017; St-Louis et al., 2014; Tuanmu and Jetz, 2015; Wood et al., 2013). The present study also showed that texture measures are useful measures for estimating the relationship between landscape heterogeneity and LST variations, and they can serve as alternatives to landscape metrics.

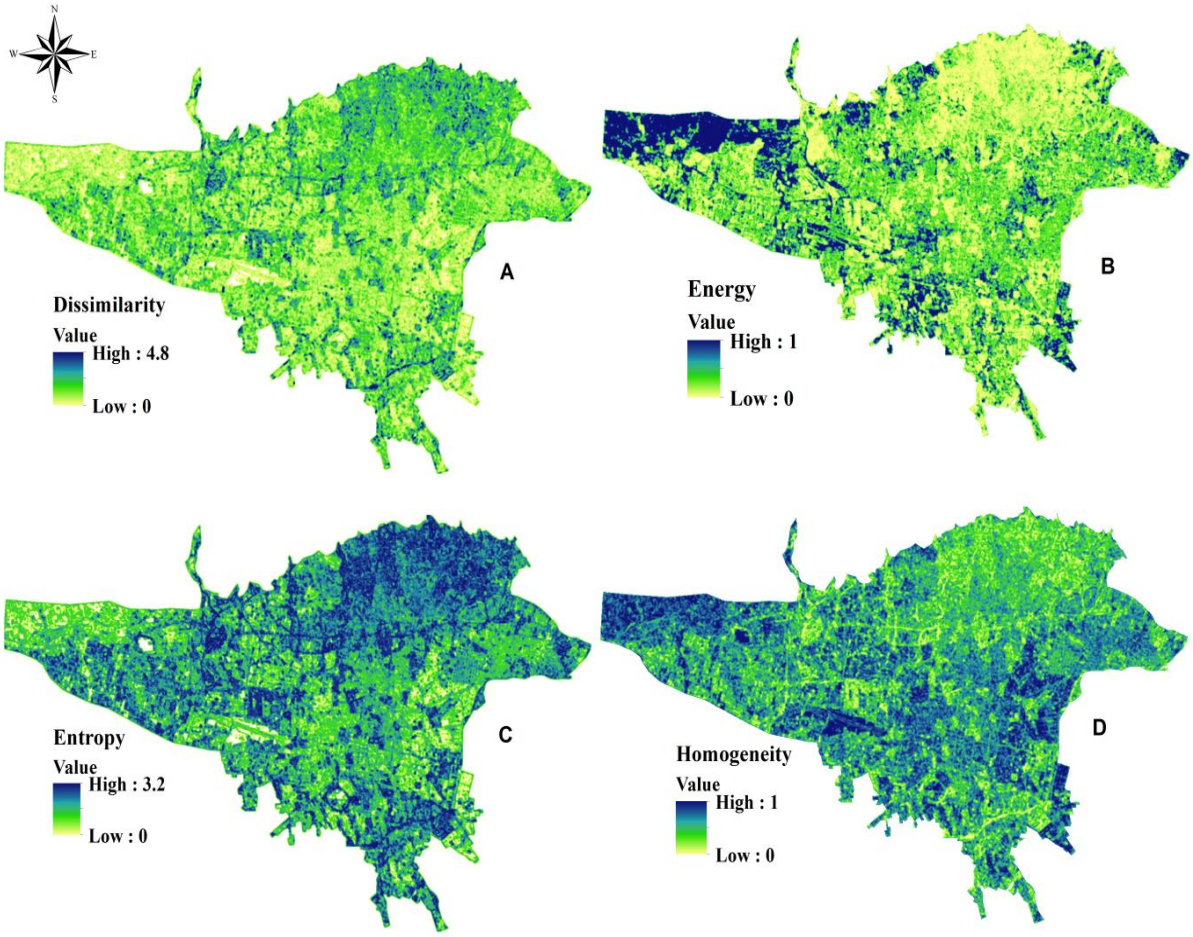

Fig. 6. Texture metrics applied to NDVI. (A) The dissimilarity of NDVI; (B) Energy of NDVI; (C) Entropy of NDVI and (D) Homogeneity of NDVI.

Conclusion

Most of the studies that have aimed to estimate the relationship between LST and landscape heterogeneity have applied landscape metrics to achieve this goal. Still, many scientists have criticized these metrics and the accuracy of their results is often controversial. This study also successfully showed that landscape metrics had some weaknesses, that one of them was the misinterpretation of the patch density (PD) metric. As shown in the current study, many studies have considered higher values of this metric as higher fragmentation and have reported their results based on this belief. However, our results showed that this belief is not always accurate and making decision merely based on confusing metrics like PD lead to unreliable consequences, so we recommend considering this critical point in future studies. Local spatial autocorrelation indices and texture measures indicated a sufficient capability to determine the relationship between landscape heterogeneity and land surface temperature. Therefore, this study suggests applying these continuous measures instead of using landscape metrics when

the spatial arrangement of landscape elements and their effects is essential. Alternative indices also have their advantages and disadvantages. For example, these indices are not easy to calculate and cannot describe functional ecological processes. Instead, using these indices saves time and is much more suitable for examining time series analysis than landscape metrics. They provide visual interpretation and can distinguish small changes in the landscape. Landscape metrics are simple and easy to calculate, they show the location of changes and are suitable for examining ecological functional processes. The most significant limitations of these metrics are; high sensitivity to input data, misinterpretations, low sensitivity to small changes, time-consuming, and budget for preparing input data.

Abbreviations

NP: Number of Patches; DIVISION: Landscape Division Index; ENN-MN: Mean Euclidean Nearest-Neighbor Distance; Area_MN: Mean Patch Area; ED: Edge Density; PAFRAC: Perimeter-Area Fractal Dimension; LSI: Landscape Shape Index; SPLIT: Splitting Index; AI: Aggregation Index;

Declarations

Ethics approval and consent to participate

Not applicable

Consent for publication

Not applicable

Competing interests

On behalf of all authors, the corresponding author states that there is no conflict of interest.

Availability of data and material

Data are available on request from the authors only based on logical requests.

Funding

There are no financial conflicts of interest to disclose.

Acknowledgment

Not applicable

Authors' contributions

Ehsan Rahimi has written the paper and has done the remote sensing analysis.
Shahindokht Barghjelveh has reviewed the paper, helped to write, and interpreted the results.
Pinliang Dong has reviewed the paper, edited grammar, and helped to compare discrete and continuous metrics.

The first author (Corresponding Author) *
Name: Ehsan
Last name: Rahimi
Address: Environmental Research Institute, Shahid Beheshti University, Tehran, Iran
E-mail*: ehsanrahimi666@gmail.com
Phone: +989379033149

Second author
Name: Shahindokht

Last name: Barghjelveh
Address: Environmental Research Institute, Shahid Beheshti University, Tehran, Iran
E-mail: shjelveh@gmail.com
Phone: +989121975296

Third author
Name: Pinliang
Last name: Dong
Address: Department of Geography and the Environment, University of North Texas, Texas, USA
E-mail: Pinliang.Dong@unt.edu
Phone: 940-565-2091, Webpage: http://geography.unt.edu/~pdong

Reference

Anselin, L., 1995, Local indicators of spatial association—LISA, *Geographical analysis* **27**(2)**:**93-115.

Asgarian, A., Amiri, B. J., Sakieh, Y., 2015, Assessing the effect of green cover spatial patterns on urban land surface temperature using landscape metrics approach, *Urban Ecosystems* **18**(1)**:**209-222.

Bao, T., Li, X., Zhang, J., Zhang, Y., Tian, S., 2016, Assessing the distribution of urban green spaces and its anisotropic cooling distance on urban heat island pattern in Baotou, China, *ISPRS International Journal of Geo-Information* **5**(2)**:**12.

Bolliger, J., Wagner, H. H., Turner, M. G., 2007, Identifying and quantifying landscape patterns in space and time, in: *A Changing World*, Springer, pp. 177-194.

Cadenasso, M. L., Pickett, S. T., Schwarz, K., 2007, Spatial heterogeneity in urban ecosystems: reconceptualizing land cover and a framework for classification, *Frontiers in Ecology and the Environment* **5**(2)**:**80-88.

Chen, A., Yao, L., Sun, R., Chen, L., 2014, How many metrics are required to identify the effects of the landscape pattern on land surface temperature?, *Ecological indicators* **45:**424-433.

Coburn, C., Roberts, A. C., 2004, A multiscale texture analysis procedure for improved forest stand classification, *International journal of remote sensing* **25**(20)**:**4287-4308.

Connors, J. P., Galletti, C. S., Chow, W. T., 2013, Landscape configuration and urban heat island effects: assessing the relationship between landscape characteristics and land surface temperature in Phoenix, Arizona, *Landscape ecology* **28**(2)**:**271-283.

Cushman, S. A., Huettmann, F., 2010, Spatial complexity, informatics, and wildlife conservation, Springer.

Dormann, C. F., 2007, Effects of incorporating spatial autocorrelation into the analysis of species distribution data, *Global ecology and biogeography* **16**(2)**:**129-138.

Essa, W., van der Kwast, J., Verbeiren, B., Batelaan, O., 2013, Downscaling of thermal images over urban areas using the land surface temperature–impervious percentage relationship, *International Journal of Applied Earth Observation and Geoinformation* **23:**95-108.

Estoque, R. C., Murayama, Y., Myint, S. W., 2017, Effects of landscape composition and pattern on land surface temperature: An urban heat island study in the megacities of Southeast Asia, *Science of the Total Environment* **577:**349-359.

Fan, C., Myint, S., 2014, A comparison of spatial autocorrelation indices and landscape metrics in measuring urban landscape fragmentation, *Landscape and Urban Planning* **121:**117-128.

Fan, C., Myint, S. W., Zheng, B., 2015, Measuring the spatial arrangement of urban vegetation and its impacts on seasonal surface temperatures, *Progress in physical geography* **39**(2)**:**199-219.

Getis, A., Ord, J. K., 1992, The analysis of spatial association by use of distance statistics, *Geographical analysis* **24**(3)**:**189-206.

Gluch, R., 2002, Urban growth detection using texture analysis on merged Landsat TM and SPOT-P data, *Photogrammetric engineering and remote sensing* **68**(12)**:**1283-1288.

Guo, G., Wu, Z., Chen, Y., 2019, Complex mechanisms linking land surface temperature to greenspace spatial patterns: Evidence from four southeastern Chinese cities, *Science of The Total Environment* **674:**77-87.

Haralick, R. M., Shanmugam, K., 1973, Textural features for image classification, *IEEE Transactions on systems, man, and cybernetics* (6)**:**610-621.

Hofmann, S., Everaars, J., Schweiger, O., Frenzel, M., Bannehr, L., Cord, A. F., 2017, Modelling patterns of pollinator species richness and diversity using satellite image texture, *PloS one* **12**(10)**:**e0185591.

Jaeger, J. A., 2000, Landscape division, splitting index, and effective mesh size: new measures of landscape fragmentation, *Landscape ecology* **15**(2)**:**115-130.

Jamei, Y., Rajagopalan, P., Sun, Q. C., 2019, Spatial structure of surface urban heat island and its relationship with vegetation and built-up areas in Melbourne, Australia, *Science of The Total Environment* **659:**1335-1351.

Kong, F., Yin, H., James, P., Hutyra, L. R., He, H. S., 2014, Effects of spatial pattern of greenspace on urban cooling in a large metropolitan area of eastern China, *Landscape and Urban Planning* **128:**35-47.

Lanorte, A., Danese, M., Lasaponara, R., Murgante, B., 2013, Multiscale mapping of burn area and severity using multisensor satellite data and spatial autocorrelation analysis, *International Journal of Applied Earth Observation and Geoinformation* **20:**42-51.

Li, J., Narayanan, R. M., 2004, Integrated spectral and spatial information mining in remote sensing imagery, *IEEE Transactions on Geoscience and Remote Sensing* **42**(3)**:**673-685.

Li, J., Song, C., Cao, L., Zhu, F., Meng, X., Wu, J., 2011, Impacts of landscape structure on surface urban heat islands: A case study of Shanghai, China, *Remote Sensing of Environment* **115**(12)**:**3249-3263.

Li, X., Zhou, W., Ouyang, Z., Xu, W., Zheng, H., 2012, Spatial pattern of greenspace affects land surface temperature: evidence from the heavily urbanized Beijing metropolitan area, China, *Landscape ecology* **27**(6)**:**887-898.

Liu, D., Hao, S., Liu, X., Li, B., He, S., Warrington, D., 2013, Effects of land use classification on landscape metrics based on remote sensing and GIS, *Environmental earth sciences* **68**(8)**:**2229-2237.

Liu, H., Weng, Q., 2008, Seasonal variations in the relationship between landscape pattern and land surface temperature in Indianapolis, USA, *Environmental Monitoring and Assessment* **144**(1)**:**199-219.

Liu, Y., Peng, J., Wang, Y., 2018, Efficiency of landscape metrics characterizing urban land surface temperature, *Landscape and urban planning* **180:**36-53.

Maimaitiyiming, M., Ghulam, A., Tiyip, T., Pla, F., Latorre-Carmona, P., Halik, Ü., Sawut, M., Caetano, M., 2014, Effects of green space spatial pattern on land surface temperature: Implications for sustainable urban planning and climate change adaptation, *ISPRS Journal of Photogrammetry and Remote Sensing* **89:**59-66.

Mallick, J., Rahman, A., Singh, C. K., 2013, Modeling urban heat islands in heterogeneous land surface and its correlation with impervious surface area by using night-time ASTER satellite data in highly urbanizing city, Delhi-India, *Advances in Space Research* **52**(4)**:**639-655.

Masoudi, M., Tan, P. Y., 2019, Multi-year comparison of the effects of spatial pattern of urban green spaces on urban land surface temperature, *Landscape and Urban Planning* **184:**44-58.

Masoudi, M., Tan, P. Y., Liew, S. C., 2019, Multi-city comparison of the relationships between spatial pattern and cooling effect of urban green spaces in four major Asian cities, *Ecological indicators* **98:**200-213.

McGarigal, K., Cushman, S. A., Neel, M. C., Ene, E., 2002, FRAGSTATS: spatial pattern analysis program for categorical maps.

Neel, M. C., McGarigal, K., Cushman, S. A., 2004, Behavior of class-level landscape metrics across gradients of class aggregation and area, *Landscape ecology* **19**(4)**:**435-455.

Nolè, G., Lasaponara, R., Lanorte, A., Murgante, B., 2014, Quantifying urban sprawl with spatial autocorrelation techniques using multi-temporal satellite data, *International Journal of Agricultural and Environmental Information Systems (IJAEIS)* **5**(2)**:**19-37.
Osborne, P. E., Alvares-Sanches, T., 2019, Quantifying how landscape composition and configuration affect urban land surface temperatures using machine learning and neutral landscapes, *Computers, Environment and Urban Systems* **76:**80-90.
Park, Y., Guldmann, J.-M., 2020, Measuring continuous landscape patterns with Gray-Level Co-Occurrence Matrix (GLCM) indices: An alternative to patch metrics?, *Ecological Indicators* **109:**105802.
Sahana, M., Ahmed, R., Sajjad, H., 2016, Analyzing land surface temperature distribution in response to land use/land cover change using split window algorithm and spectral radiance model in Sundarban Biosphere Reserve, India, *Modeling Earth Systems and Environment* **2**(2)**:**81.
Shao, G., Wu, J., 2008, On the accuracy of landscape pattern analysis using remote sensing data, *Landscape Ecology* **23**(5)**:**505-511.
Sodoudi, S., Shahmohamadi, P., Vollack, K., Cubasch, U., Che-Ani, A., 2014, Mitigating the urban heat island effect in megacity Tehran, *Advances in Meteorology* **2014**.
St-Louis, V., Pidgeon, A. M., Kuemmerle, T., Sonnenschein, R., Radeloff, V. C., Clayton, M. K., Locke, B. A., Bash, D., Hostert, P., 2014, Modelling avian biodiversity using raw, unclassified satellite imagery, *Philosophical Transactions of the Royal Society of London B: Biological Sciences* **369**(1643)**:**20130197.
Tuanmu, M. N., Jetz, W., 2015, A global, remote sensing-based characterization of terrestrial habitat heterogeneity for biodiversity and ecosystem modelling, *Global ecology and biogeography* **24**(11)**:**1329-1339.
Turner, M. G., Gardner, R. H., O'neill, R. V., 2001, Landscape ecology in theory and practice, Springer.
Tuttle, E. M., Jensen, R. R., Formica, V. A., Gonser, R. A., 2006, Using remote sensing image texture to study habitat use patterns: a case study using the polymorphic white-throated sparrow (Zonotrichia albicollis), *Global Ecology and Biogeography* **15**(4)**:**349-357.
Wood, E. M., Pidgeon, A. M., Radeloff, V. C., Keuler, N. S., 2013, Image texture predicts avian density and species richness, *PloS one* **8**(5)**:**e63211.
Xie, M., Wang, Y., Chang, Q., Fu, M., Ye, M., 2013, Assessment of landscape patterns affecting land surface temperature in different biophysical gradients in Shenzhen, China, *Urban Ecosystems* **16**(4)**:**871-886.
Yang, X., Li, J., 2012, Advances in mapping from remote sensor imagery: techniques and applications, CRC Press.
Yue, W., Xu, J., Tan, W., Xu, L., 2007, The relationship between land surface temperature and NDVI with remote sensing: application to Shanghai Landsat 7 ETM+ data, *International Journal of Remote Sensing* **28**(15)**:**3205-3226.
Zhang, X., Zhong, T., Feng, X., Wang, K., 2009, Estimation of the relationship between vegetation patches and urban land surface temperature with remote sensing, *International Journal of Remote Sensing* **30**(8)**:**2105-2118.
Zhang, Y., Odeh, I. O., Ramadan, E., 2013, Assessment of land surface temperature in relation to landscape metrics and fractional vegetation cover in an urban/peri-urban region using Landsat data, *International journal of remote sensing* **34**(1)**:**168-189.
Zheng, B., Myint, S. W., Fan, C., 2014, Spatial configuration of anthropogenic land cover impacts on urban warming, *Landscape and Urban Planning* **130:**104-111.
Zhibin, R., Haifeng, Z., Xingyuan, H., Dan, Z., Xingyang, Y., 2015, Estimation of the relationship between urban vegetation configuration and land surface temperature with remote sensing, *Journal of the Indian Society of Remote Sensing* **43**(1)**:**89-100.
Zhou, W., Huang, G., Cadenasso, M. L., 2011, Does spatial configuration matter? Understanding the effects of land cover pattern on land surface temperature in urban landscapes, *Landscape and Urban Planning* **102**(1)**:**54-63.

676

Figures

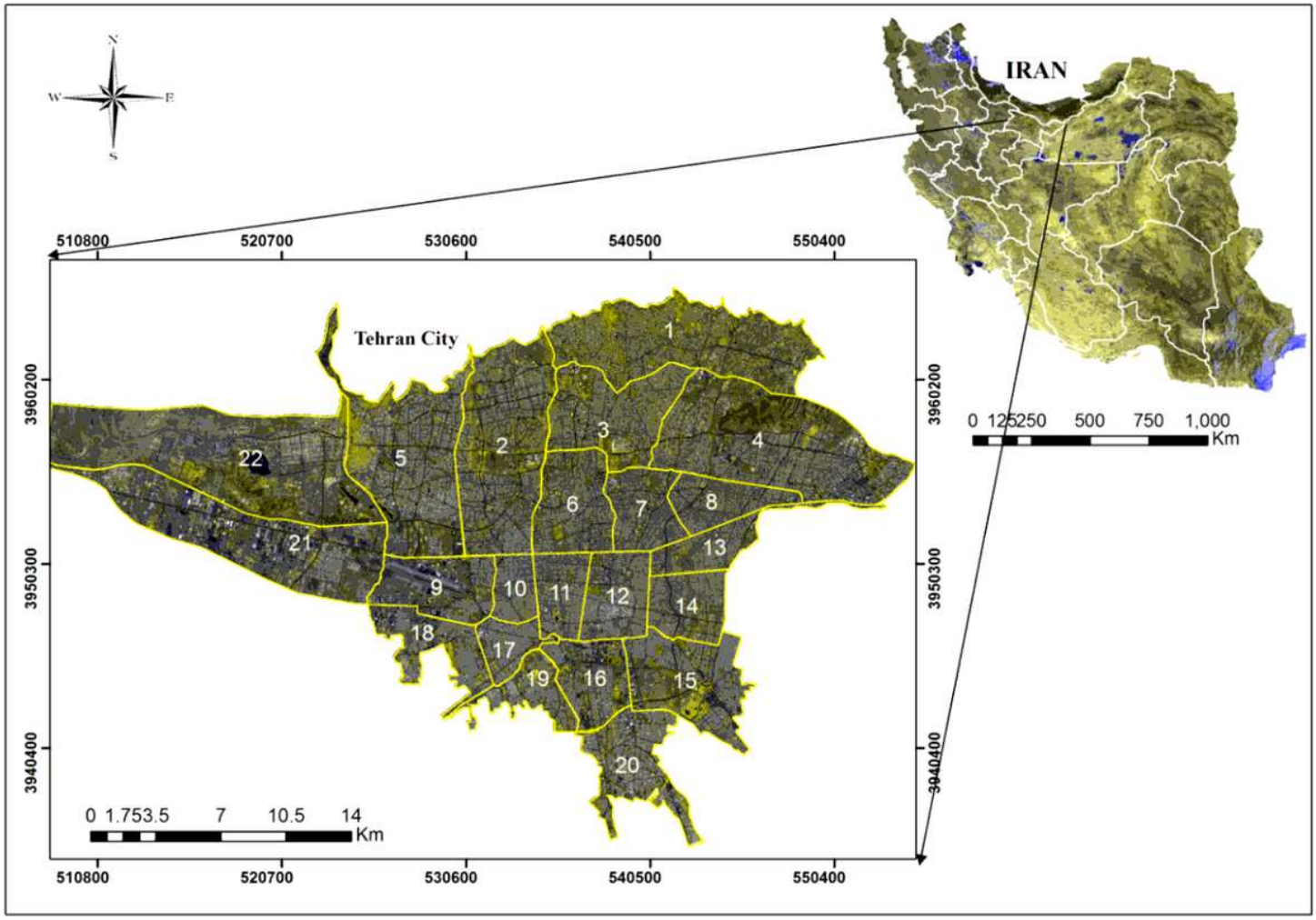

Figure 1

Study area location in Tehran province and Iran. Note: The designations employed and the presentation of the material on this map do not imply the expression of any opinion whatsoever on the part of Research Square concerning the legal status of any country, territory, city or area or of its authorities, or concerning the delimitation of its frontiers or boundaries. This map has been provided by the authors.

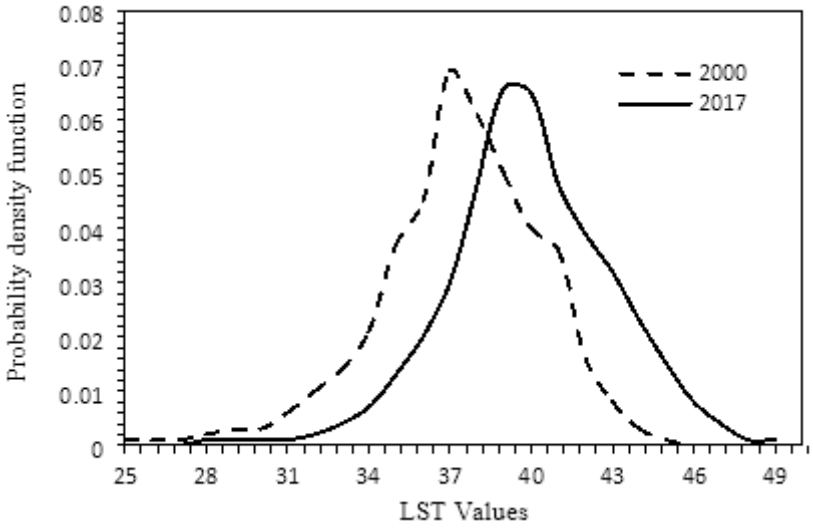

Figure 2

Density function applied to LST maps in 2000 and 2017.

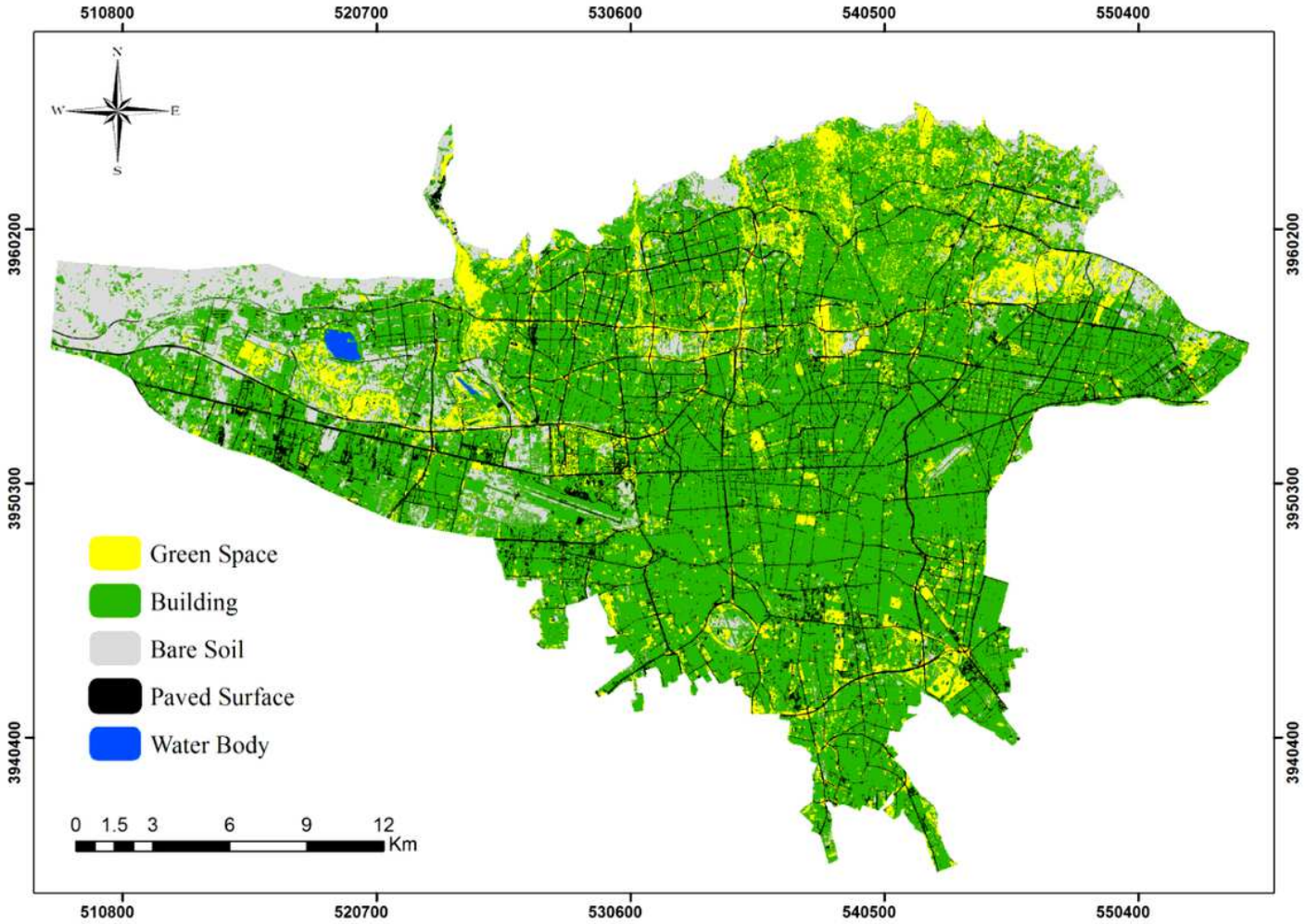

Figure 3

Land cover map of the study area in 2017. Note: The designations employed and the presentation of the material on this map do not imply the expression of any opinion whatsoever on the part of Research Square concerning the legal status of any country, territory, city or area or of its authorities, or concerning the delimitation of its frontiers or boundaries. This map has been provided by the authors.

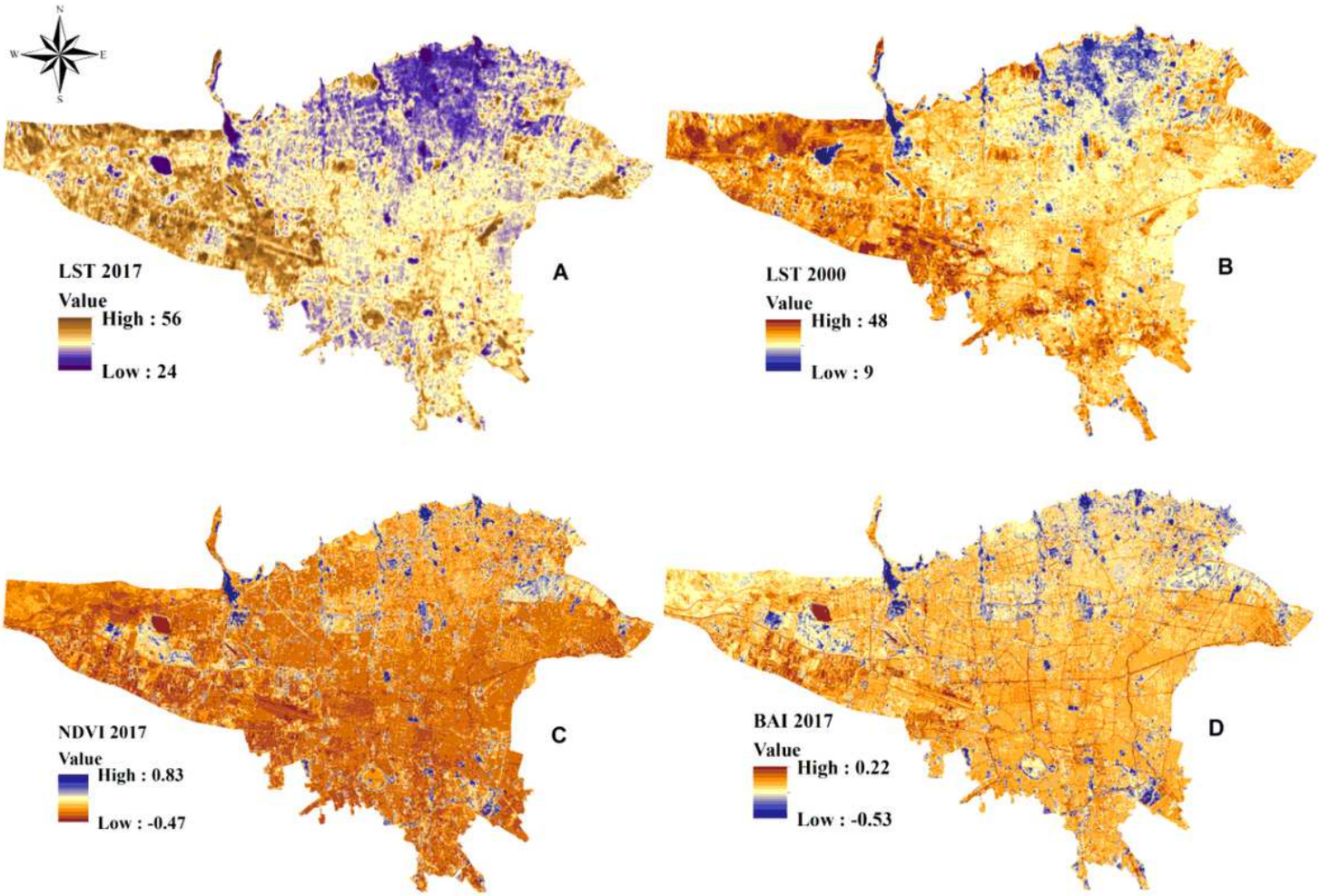

Figure 4

LST maps in (A) 2017, (B) 2000, (C) NDVI, and (D) BAI indices. Note: The designations employed and the presentation of the material on this map do not imply the expression of any opinion whatsoever on the part of Research Square concerning the legal status of any country, territory, city or area or of its authorities, or concerning the delimitation of its frontiers or boundaries. This map has been provided by the authors.

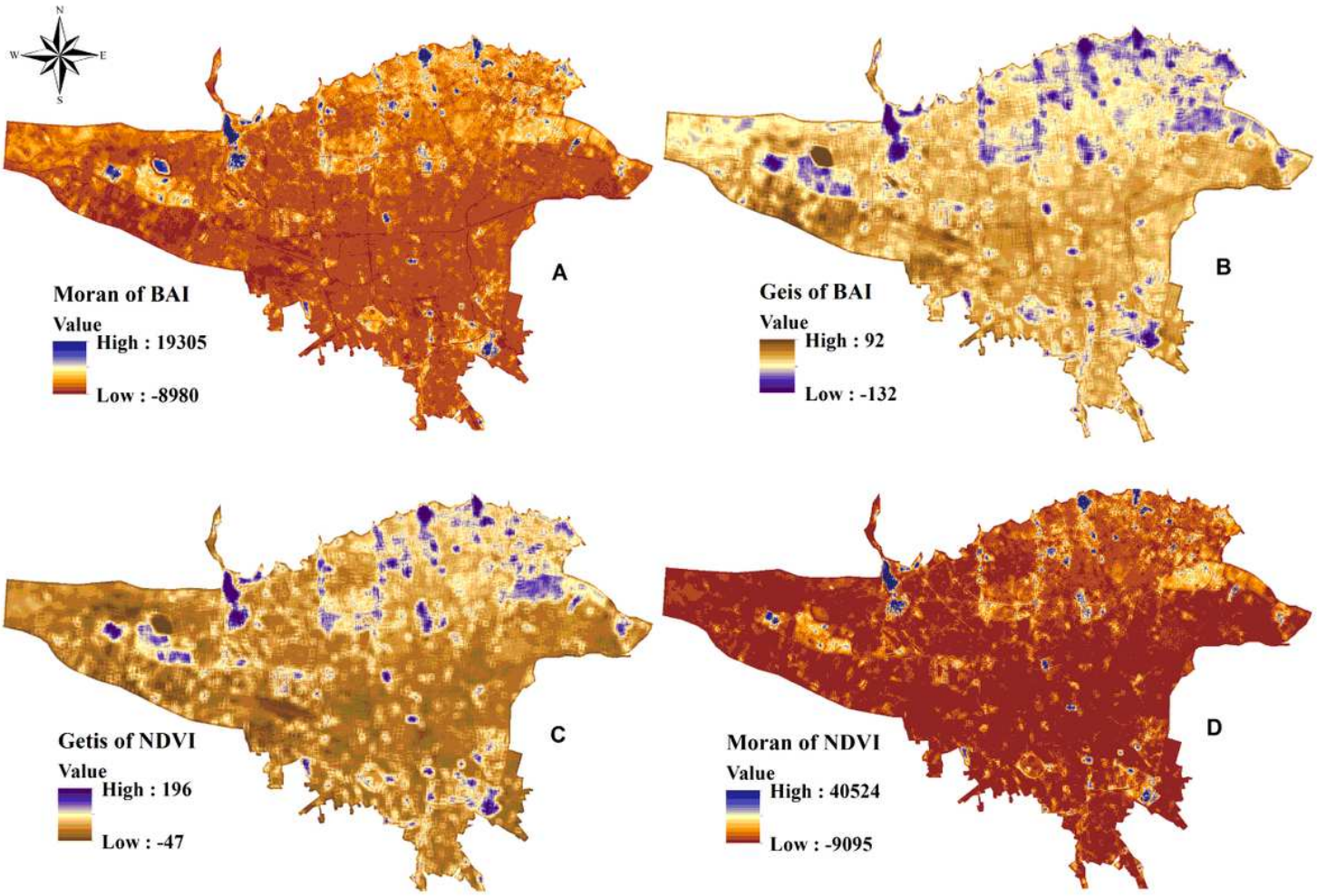

Figure 5

Local spatial autocorrelation indices applied to NDVI and BAI indices. (A) Moran of BAI, (B) Getis of BAI, (C) Getis of NDVI, and (D) Moran of NDVI. Note: The designations employed and the presentation of the material on this map do not imply the expression of any opinion whatsoever on the part of Research Square concerning the legal status of any country, territory, city or area or of its authorities, or concerning the delimitation of its frontiers or boundaries. This map has been provided by the authors.

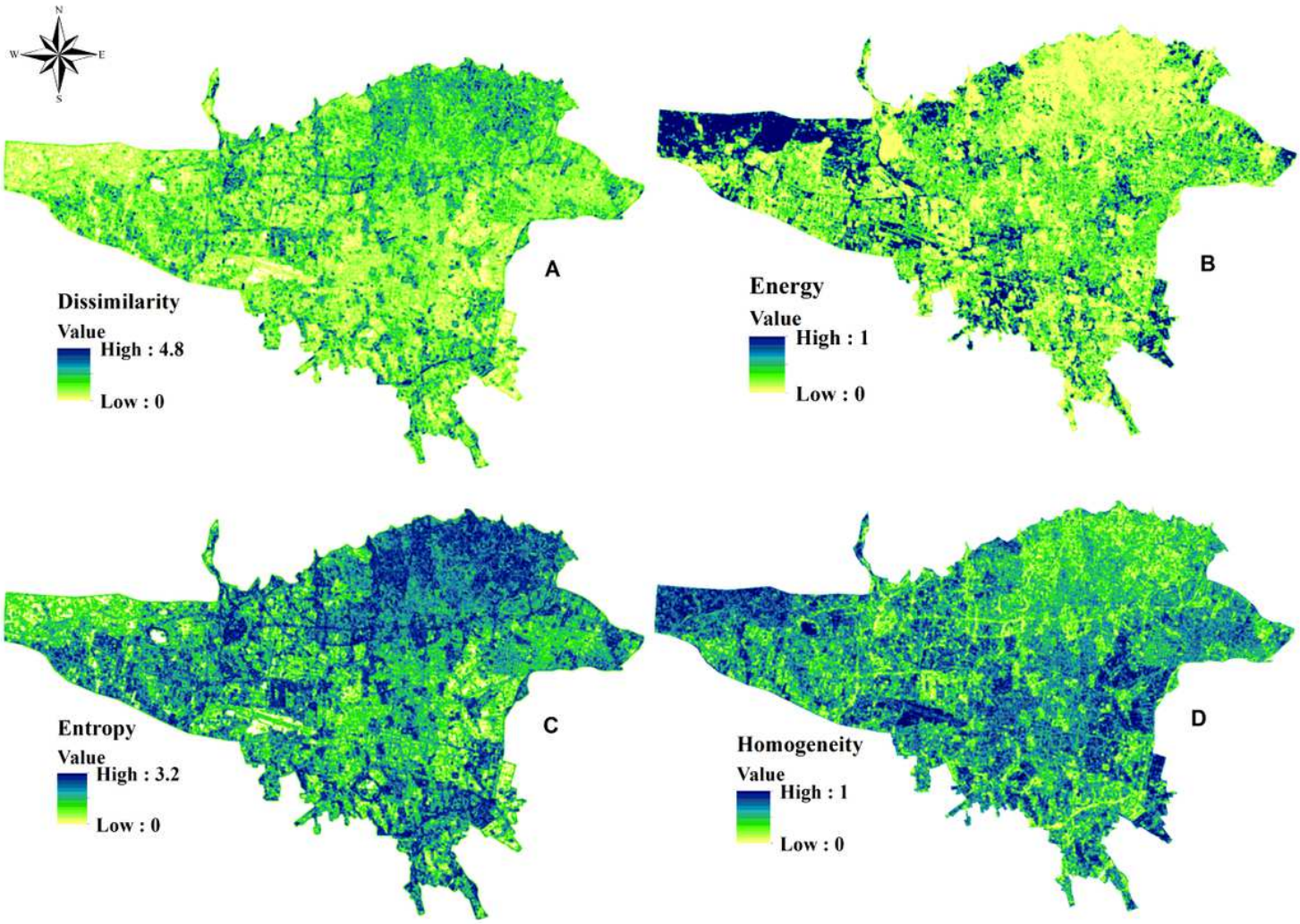

Figure 6

Texture metrics applied to NDVI. (A) The dissimilarity of NDVI; (B) Energy of NDVI; (C) Entropy of NDVI and (D) Homogeneity of NDVI. Note: The designations employed and the presentation of the material on this map do not imply the expression of any opinion whatsoever on the part of Research Square concerning the legal status of any country, territory, city or area or of its authorities, or concerning the delimitation of its frontiers or boundaries. This map has been provided by the authors.